Finite Element Analyses for a Study of Hepatic Cancer Tissue Destruction using Monopolar and Bipolar Radio-Frequency Ablation

Supan Tungjitkusolmun, Member

ABSTRACT

This paper presents three-dimensional finite element analyses of radio-frequency hepatic tumor ablation. The analyses performed in this paper are composed of two systems. In the first system, the simulation was of monopolar ablation (one needle), while the second system was the simulation of bipolar ablation (two needles). We performed a preliminary study of thermal and electrical distributions of both systems. Additional simulations of bipolar ablation were performed to investigate the effect of spacing distance between two needle electrodes (2 cm, 3 cm, 4 cm, and 5 cm). The ablation duration used in all cases was 10 min, and the controlled maximum temperature was set to 90 °C. From the results, the electric field in monopolar ablation appeared to be distributed uniformly between the electrode and the ground surface, but the electric field in bipolar ablation was focused in the regions between the two electrodes. For bipolar ablation, when the distances between the electrodes were 2 cm and 3 cm, the lesion created was contiguous and covered the areas surrounding both electrodes. However, when the distances between the electrodes were 4 cm and 5 cm, the lesions created were not contiguous and shaped similar to performing two monopolar ablation operations.

Keywords: three-dimensional, finite element, bipolar, radio-frequency, cancer tissue, hepatic

1. INTRODUCTION

Every year, more than one million people around the world die with hepatocellular carcinoma (HCC). Thus, it is one of the challenging problems for the medical community [1]. Possible treatments for primary hepatic cancers are surgical operation, chemical treatment, cryoablation, radiation therapy, and radio-frequency (RF) ablation [2]. Currently, surgical resection is the treatment of choice for both well-localized primary and metastatic hepatic malignancies. However, the majority of the patients are not candidates for surgical resection due to restrictions, such as multifocal disease, tumor size, location of tumor to key vessels, or coagulopathies. Chemical treatment, where adequate chemical injection is administered into artery supplying cancer tissues, and radiation therapy are mostly used to temporarily relieve the symptoms. A combination of the above methods has also been used for treatment of hepatic cancer to improve the degree of success.

RF ablation has been recently introduced and has proved to be an effective cure for primary hepatic cancer where the tumors found are still small (< 3 cm in diameter) [2]. In RF ablation, electric current at frequencies between 350-500 kHz is passed into cancer cells via an electrode placed inside the tumor. The electric energy generates Joule heat which then conducts into surrounding tissues. Elevating temperature of unwanted tissues to a level above 50 °C can effectively kill cancer cells. RF ablation is much less invasive compared to surgical resection as only a small incision is required for insertion of ultrasound-guided RF probe. Thus RF ablation reduces risks of side effects and requires less recovery period for patients [9-23].

Commonly reported disadvantages in RF ablation technique include difficulty in treating large tumors-that is, those exceeding 3 cm in diameter; the potential for incomplete RF tumor ablation near blood vessels because of the heat sink effect of local blood flow, difficulty in obtaining sonographic images of RF lesions; and evidence of surviving tumor cells, even within RF lesions. Treatment of large tumors by performing sequential RF ablations can be time consuming to adequately ensure total overlapping coverage of the ablation zones. Proposed modifications of the conventional RF ablation technique to increase lesion dimensions include injecting cool saline at the distal end of the probes to reduce overheating at regions in close proximity to avoid a sudden increase in impedance, using multiple tines which can increase effective heating area, and the use of multiple RF probes to achieve larger coagulation volumes than those possible with a single probe.

Commonly reported disadvantages in RF ablation

Manuscript received on June 15, 2009 ; revised on July 15, 2009.

S. Tungjitkusolmun is with Department of Electronics, Faculty of Engineering, King Monkut's Institute of Technology Ladkrabang, Bangkok, Thailand

E-mail address: ktsupan@gmail.com

technique include difficulty in treating large tumors-that is, those exceeding 3 cm in diameter; the potential for incomplete RF tumor ablation near blood vessels because of the heat sink effect of local blood flow, difficulty in obtaining sonographic images of RF lesions; and evidence of surviving tumor cells, even within RF lesions. Treatment of large tumors by performing sequential RF ablations can be time consuming to adequately ensure total overlapping coverage of the ablation zones. Proposed modifications of the conventional RF ablation technique to increase lesion dimensions include injecting cool saline at the distal end of the probes to reduce overheating at regions in close proximity to avoid a sudden increase in impedance, using multiple tines which can increase effective heating area, and the use of multiple RF probes to achieve larger coagulation volumes than those possible with a single probe.

2. METHODOLOGY

Mathematical modeling is a powerful tool for predicting lesion dimensions created by various RF probe designs. In order to know the change in potential and temperature distributions in the hepatic tissue during ablation, we solved the bio-heat equation. As the geometries of the objects involved in RF hepatic ablation (RF probe, blood vessels, hepatic tissue) are complicated, we performed the FE method to solve the bio-heat equation.

Three-dimensional FE [5] analyses were used in this study. The procedure was used to determine the temperature distribution that happened from coagulation of liver cancer. Our system was consisted of four materials electrode, catheter body, liver cancer, and normal liver tissue. In RF ablation, electric energy acts as a heat source flowing from the ablation electrode into tissue. Thus, we used the bioheat equation to determine the thermal-electrical effect within the domain of our system. Detailed information for the bioheat equation and our three-dimensional finite element models will be described in this section.

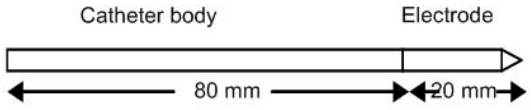

Fig.1: *CThe dimensions for electrode and catheter body. The diameter of the electrode was 2 mm.*

2.1 The Bioheat Equation

The mechanism by which RF current induces tissue injury is the conversion of electric energy into heat. The circuit consists of the RF generator, the connecting wire to the distal electrodes, liver (and other tissues in the abdomen), a surface dispersive electrode, and the connecting wires to the generator that will close the electric circuit. Joule heating arises when energy dissipated by an electric current flowing through a conductor is converted into thermal energy.

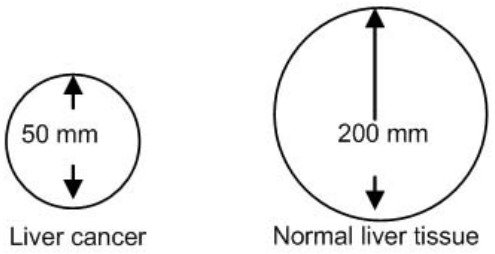

Fig.2: *Sizes of liver cancer and normal liver tissue*

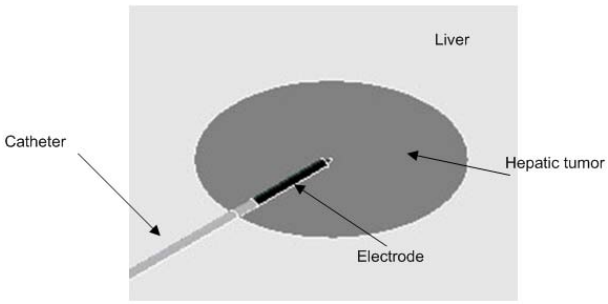

Fig.3: *Cross sectional geometries of the monopolar RFA*

The bioheat equation below was employed to analyze heat generation from electric energy [6]. We solved the bioheat equation to obtain the thermal distribution in hepatic cancer tissue and normal liver tissue.

$$\rho c\frac{\partial T}{\partial t} = \nabla.\kappa\nabla T + J.E - h_{b1}(T - T_{b1}) - Q_m$$

$$h_{b1} = \rho_{b1}c_{b1}\omega_{b1}$$

ρ	=	Density(kg/m^3)
c	=	Specific heat (J/kg K)
k	=	Thermal conductivity (W/m·K)
J	=	Current density (A/m^2)
E	=	Electric field intensity (V/m)
T_{b1}	=	Temperature of the blood (assumed to be 37 °C)
ρ_{b1}	=	The blood density (kg/m^3)
c_{b1}	=	Specific heat of the blood(J/kg·K)
ω_{b1}	=	blood perfusion (1/s)
h_{b1}	=	The convective heat transfer coefficient accounting for blood perfusion in the model
Q_m		The energy generated by the metabolic processes (W/m^3)

Table 1: *Material properties at the frequency 500 kHz*

FEM region	Material	ρ[Kg/m^3]	c[J/kg.K]	k[W/m.K]	σ[S/m]
Electrode	Ni-Ti	6,450	840	18	1×10^8
Tissue	Liver	1,060	3,600	0.512	0.300
Tissue	Hepatic Tumor	1,060	3,600	0.512	0.400
Catheter body	Polyurethane	70	1,045	0.026	10^{-5}

Since Q_m is negligible, we excluded it from our FE models. We also omitted h_{b1} from our preliminary studies.

2.2 Material Properties

We used the material properties required for electrode, catheter body, liver cancer, and normal liver tissue at approximately 500 kHz. Table 1 summarizes the material properties included in our 3-D FE models, such as density (kg/m^3), specific heat (J/kg·K), thermal conductivity (W/m·K), electrical conductivity [S/m] [5], [7].

2.3 Software

We constructed the geometrical model, assigned material properties to the appropriate regions, and ran all numerical simulations using ANSYS 5.7. We ran our simulations on a PC with Intel Pentium IV 2.4 GHz, and 512 MB of RAM.

2.4 4Three-dimensional FE analyses for hepatic ablation

Figure 1 shows the typical geometries of the electrode in our FE models. The electrode was 2-mm in diameter, and 20 mm in length. The catheter body was 80 mm long. In Figure 2, the shape of hepatic tumor was spherical (50 mm in diameter), while the shape of liver tissue was spherical (200 mm in diameter), encompassing the hepatic tumor. Figure 3 shows the cross sectional geometries of the monopolar RFA. For bipolar ablation, we added another identical RFA electrode to the monopolar model.

We performed 3-D FE analyses for the following cases:

(Case 1) Monopolar RFA
(Case 2) The two electrodes were parallel, with spacing distance of 20 mm (bipolar RFA-20 mm).
(Case 3) The two electrodes were parallel with spacing distance of 30 mm (bipolar RFA-30 mm).
(Case 4) The two electrodes were parallel, with spacing distance of 40 mm (bipolar RFA-40 mm).
(Case 5) The two electrodes were parallel with spacing distance of 50 mm

The five cases were simulated using 3-D FE models. The monopolar electrode was assigned with an electric potential, while the outer most surface was ground. For the bipolar model, an electrical potential was assigned at one electrode, while the other electrode was treated as ground. We performed temperature controlled ablation of 90°C that is, the maximum tissue temperature allowed in the model was set to 90 °C. The tissue lesion was defined as regions with temperature over 50 °C.

3. RESULTS

3.1 Monopolar RFA (Case 1)

Figure 4 shows the cross-section temperature distribution and the extent of the lesion formation after 10 min, 90 °C in liver tissue. The Joule Heat conducted out of electrode into surrounding tissues. The temperatures where lesion formation occurred were considered to be between 50 °C to 90 °C. The shape of the lesion was ellipsoidal and appeared to be symmetric along the axis of the monopolar needle.

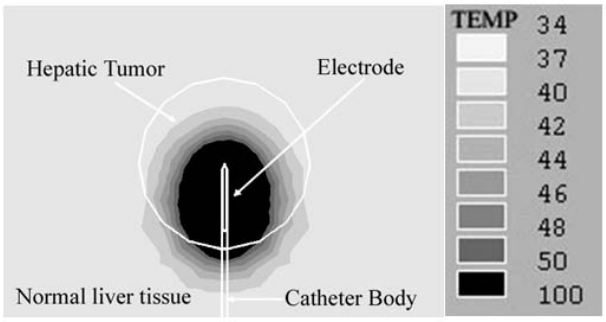

Fig.4: *The cross-section temperature distribution for FEM analysis in (Case 1).*

3.2 3-D FEM bipolar model with two parallel needle electrodes with 2 cm spacing (Case 2)

Figure 5 shows cross sectional temperature distribution and the extent of lesion formation after 10 min, 90 °C in liver tissue. The lesion was created between the two electrodes, covering most of the tumor and parts of normal liver tissue. The maximum temperature occurred around the tips of both electrodes.

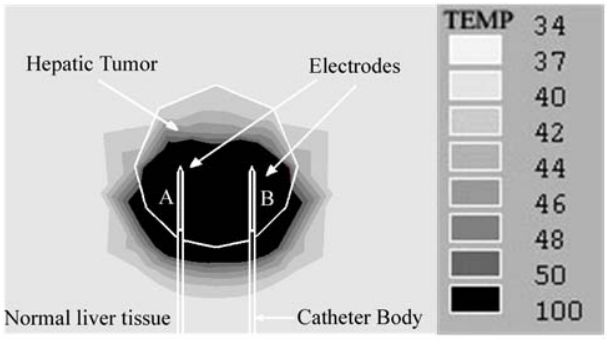

Fig.5: *The cross-section temperature distribution for FEM analysis in (Case 2).*

3.3 3-D FEM bipolar model with two parallel needle electrodes with 3 cm spacing (Case 3)

Figure 6 shows cross sectional temperature distribution for (Case 3) where the electrodes were placed 3 cm apart. Similar to (Case 2), a contiguous lesion was formed between the two electrodes with maximum temperatures situating around the electrode tips. The shape of the lesion is butterfly-like with a narrower region in the middle. The total lesion width in this case was 58.85 mm which was higher than the previous two cases.

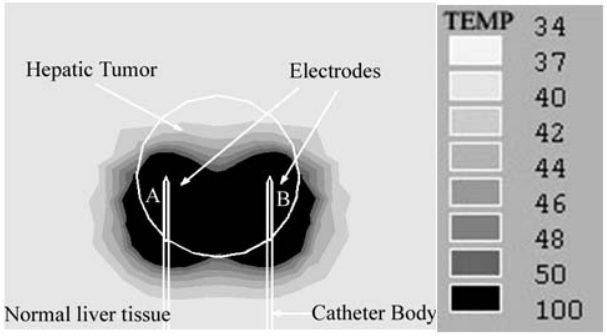

Fig.6: *The cross-section temperature distribution for FEM analysis in (Case 3).*

3.4 3-D FEM bipolar model with two parallel needle electrodes with 4 cm spacing (Case 4)

Figure 7 shows the cross sectional temperature distribution and the extent of lesion formation for (Case 4) where the bipolar electrodes were 4 cm apart. In contrast to (Case 3), the lesions formed in this case were not contiguous between the two electrodes but separated into two regions surrounding each electrodes.

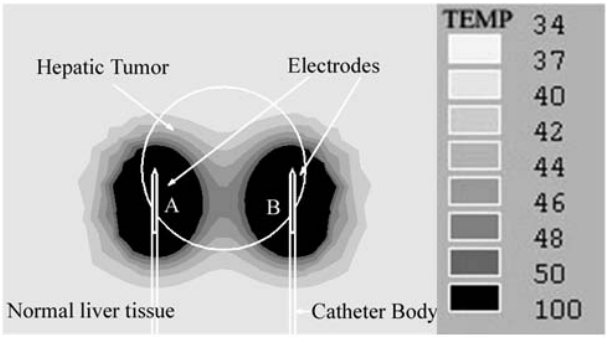

Fig.7: *cross-section temperature distribution for FEM analysis in (Case 4).*

3.5 3-D FEM bipolar model with two parallel needle electrodes with 2 cm spacing (Case 5)

Figure 8 shows the cross sectional temperature distribution and the extent of lesion formation for (Case 5) where the bipolar electrodes were 5 cm apart. Similar to the previous case (Case 4), the lesions formed in this case were not contiguous between the two electrodes but separated into two regions surrounding each electrodes. A large portion of the lesion formed was in the liver tissue, instead of the tumor.

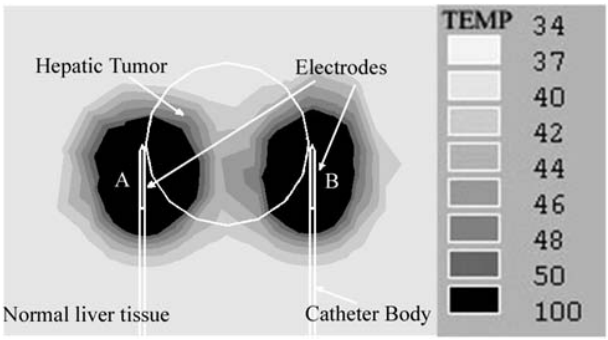

Fig.8: *The cross-section temperature distribution for FEM analysis in (Case 5).*

Figure 9 illustrates the distances measured (D1 to D8) for the extent of lesion formed around each electrode. A1 is distance between the two parallel electrodes. Parameters A1 in (Case 2) to (Case 5) are 2cm, 3cm, 4cm, 5cm, respectively. Table 2 lists the distances of lesion formed in electrode one (on the left). Each distance was measured from the middle point of the 20 mm electrode. The distances (D1-D8) around electrode two (right) are listed in Table 3 for each case.

From the parameters in Table 2 and 3, the lesion depths (D1) for each case did not vary significantly (16.47 to 19.55 mm) while the lesion widths for Case 3 was largest with combined distance (D3+D7 of both

Table 2: *Extent of lesion formation for electrode 1*

Case	D1(mm)	D2(mm)	D3(mm)	D4(mm)	D5(mm)	D6(mm)	D7(mm)	D8(mm)
1	17.05	15.19	13.3	15.82	17.8	15.52	13.6	16.8
2	17.85	20.5	11.25	22.41	18.4	15.1	15.05	15.39
3	16.9	16.86	15.85	20.11	18.5	15.53	13.15	14.34
4	17.1	15.47	14.55	15.77	17.25	15.07	12.6	15.25
5	18.7	19.5	17.56	16.83	17.55	15.18	13.83	17.65

Table 3: *Extent of lesion formation for electrode 2*

Case	D1(mm)	D2(mm)	D3(mm)	D4(mm)	D5(mm)	D6(mm)	D7(mm)	D8(mm)
1	-	-	-	-	-	-	-	-
2	18.15	15.03	15.05	14.57	18.35	22.21	10.9	20.7
3	16.5	13.83	13.6	16.18	18.7	19.74	16.15	16.57
4	16.47	14.87	12.55	15.24	17.3	16.43	14.7	15.72
5	19.55	19.02	13.37	14.7	18	16.85	15.25	17.65

electrodes) of 58.85 mm. In case 2, the lesion was also contiguous with a lesion width of 52.25 mm. For monopolar ablation, the lesion width was 26.9 mm, while the lesion depth was comparable to that of bipolar ablation.

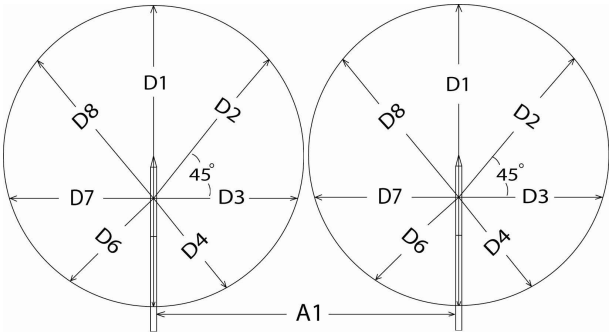

Fig.9: *Diagram of the distance parameters measured for lesion formation of electrode 1 and 2.*

4. CONCLUSION

The bioheat equation was employed to analyze heat generation from electric energy. The thermal conduction occurred in both monopolar electrode and bipolar electrode. Bipolar ablations were able to create larger lesions as temperature rose in regions surrounding both electrodes. Thus, bipolar ablation has a potential for large area of tissue destruction. For bipolar ablation with spacing distance of 2 cm or 3 cm, the lesion was contiguously formed between the two electrodes. When we increased the spacing distance to 4 cm and 5 cm, the lesions formed were no longer contiguous. Instead, the lesions created were similar to two monopolar lesions. Thus, although bipolar ablation is able to create larger lesions than monopolar ablation, spacing distance between the two electrodes plays a major role in determining the characteristics of lesions. For full thickness and continuous tissue destruction, a spacing distance of approximately 3 cm appears to be optimal. The authors plan to compare simulation results with in vitro experiments as well as experiment with more complex electrode configurations.

References

[1] S. A. Curley, F. Izzo, P. Delrio, L. M. Ellis, J. Granchi, P. Vallone, F. Fiore, S. Pignata, B. Banielle, and F. Cremona, "Radiofrequency ablation of unresectable primary and metastatic hepatic malignancies: Results in 123 patients," *Ann. Surgery,* vol. 230, pp. 1 8, 1999.

[2] J. P. McGahan, J. M. Brock, H. Tesluk, W.-Z. Gu, P. Schneider, and P. D. Browing, "Hepatic ablation with use of radio-frequency electrocautery in the animal model," *J. Vasc. Inter. Radiol.,* vol. 3, pp. 291 297, 1992.

[3] T. Livraghi, S. N. Goldberg, F. Monti, A. Bizzini, S. Lazzaroni, F. Meloni, S. Pellicano, L. Solbiati, and G. S. Gazelle, "Saline-enhanced radiofrequency tissue ablation in the treatment of liver metastases," *Radiology,* vol. 202, pp. 205 210, 1997.

[4] S. Rossi, E. Buscarini, R. Garbagnati, M. Di Stasi, P. Quaretti, M. Rago, A. Zangrandi, S. Andreola, D. Silverman, L. Buscarini, "Percutaneous treatment of small hepatic tumors by an expandable RF needle electrode," *Am. J. Radiology,* vol. 170, pp. 1015 1022, 1998.

[5] S. Rossi, M. Di Stasi, E. Buscarini, P. Quaretti, F. Garbagnati, L. Squassante, C. T. Paties, D. E. Silverman, and L. Buscarini, "Percutaneous RF interstitial thermal ablation in the treatment of hepatic cancer," *Am. J. Roentgenol.,* vol. 167, pp. 759 768, 1996.

[6] L. R. Jiao, P. D. Hansen, R. Havlik, R. R. Mitry, M. Pignatelli, N. Habib, "Clinical short-term results of radiofrequency ablation in primary and secondary liver tumors," *Am. J. Surgery,* vol. 177, pp. 303 306, 1999.

[7] S. H. Landis, T. Murray, S. Bolden, P. A. Wingo,

"Cancer Statistics 1999," *CA: Cancer J. Clin.* vol. 49, pp. 8 31, 1999.

[8] L. Solbiati, T. Ierace, S. N. Goldberg, S. Sironi, T. Livraghi, R. Fiocca, G. Servadio, G. Rizzatto, P. R. Mueller, A. Del Maschio, and G. S. Gazelle, "Percutaneous US-guided radiofrequency tissue ablation of liver metastases: treatment and follow-up in 16 patients," *Radiology,* vol. 202, pp. 195 203, 1997.

[9] D. Panescu, J. G. Whayne, S. D. Fleischman, M. S. Mirotznik, D. K. Swanson, and J. G. Webster, "Three-dimensional finite element analysis of current density and temperature distributions during radio-frequency ablation," *IEEE Trans. Biomed. Eng.,* vol. 42, pp. 879 890, 1995.

[10] S. Tungjitkusolmun, E. J. Woo, H. Cao, J. Tsai, V. R. Vorperian, and J. G. Webster, "Thermal-electrical finite element modeling for radio-frequency cardiac ablation: effects of changes in myocardial properties," *Med. Biol. Eng. Comput., submitted.,* 1999.

[11] S. Tungjitkusolmun, E. J. Woo, H. Cao, J.-Z. Tsai, V. R. Vorperian, and J. G. Webster, "Finite element analyses of uniform current density electrodes for radio-frequency cardiac ablation," *IEEE Trans. Biomed. Eng.,* vol. 47, pp. 32 40, 2000.

[12]] M. G. Curley, and P. S. Hamilton, "Creation of large thermal lesions in liver using saline-enhanced RF ablation," *Proc. 19th Annu. Int. Conf. IEEE Eng. Med. Biol. Soc. (Chicago, 1997) (Piscataway, NJ: IEEE),* pp. 2516 2519.

[13] J. Chato, "Heat transfer to blood vessels," *ASME Trans. Biomech. Eng.,* vol. 102, pp. 110 118, 1980.

[14] J. W. Valvano, J. R. Cochran, and K. R. Diller, "Thermal conductivity and diffusivity of biomaterials measured with self-heating thermistors", *Int. J. Themophys.,* vol. 6, pp. 301 311, 1985.

[15] T. E. Cooper, and G. J. Trezek, "A probe technique for determining the thermal conductivity of tissue," *J. Heat Transfer, Trans. ASME.,* vol. 94, pp. 133 140, 1972.

[16] E. S. Ebbini, S.-I. Umemura, M. Ibbini, and C. A. Cain, "A cylindrical-section ultrasound phased-array applicator for hyperthermia cancer therapy," *IEEE Trans. Ultrasonics, Ferroelectrics and Frequency Control.,* vol. 35, pp. 561 572, 1988.

[17] S. N. Goldberg, G. S. Gazelle, L. Solbiati, T. Livraghi, K. K. Tanabe, P. F. Hahn, and P. R. Mueller, "Ablation of liver tumors using percutaneous RF therapy," *Am. J. Roentgenol.,* vol. 170, pp. 1023 1028, 1998.

[18] Y. Miao, Y. Ni, S. Mulier, K. Wang, M. Hoey, P. Mulier, F. Penninckx, J. Yu, I. De Scheerder, A. L. Baert, and G. Marchal, "Ex vivo experiment on radiofrequency liver ablation with saline infusion through a screw-tip cannulated electrode," *J. Surg. Res.,* vol. 71, pp. 19 24, 1997.

[19] C. O. Esquivel, E. B. Keeffe, G.Garcia, J.C.Imperial, M.Millan, H.Monge, and S. K. So, "Hepaticneoplasms: Advances in treatment," *J. Gastroenterol. Hepatol.,* vol. 14 (suppl.), pp. 37-41, 1999.

[20] P. Liang, B. Dong, X. Yu, D. Yu, Z. Cheng, L. Su, J. Peng, Q. Nan, and H. Wang, "Computer-Aided Dynamic Simulation of Microwave-Induced Thermal Distribution in Coagulation of Liver Cancer," *IEEE Trans. Biomed. Eng,* vol.48, no.7, pp. 821-829, 2001

[21] J. M. Lee, J. K. Han, S. H. Kim, K. H. Lee, S. K. Ah, B. Choi, "A Comparative Experimental Study of the In-vitro Efficiency of Hypertonic Saline-Enhanced Hepatic Bipolar and Monopolar Radiofrequency Ablation," *KOREAN J Radiol,* 4(3), pp.163-169, 2003.

[22] Highfrequency induced thermotherapy (HiTT) ELEKTROTOMHiTT106 http://www.BERCHTOLD.de

[23] S. Tungjitkusolmun, S.T. Staelin, D. Haemmerich, Jang-Zern Tsai; Hong Cao; J.G. Webster, F.T. Lee, Jr, D.M. Mahvi, V.R. Vorperian, "Three-Dimensional Finite-Element Analyses for Radio-Frequency Hepatic Tumor Ablation," *IEEE Trans. Biomed. Eng,* vol.49, no.1, pp.3-9, 2002.

[24] J. Chato, "Heat transfer to blood vessels," *ASME Trans. Biomech. Eng.,* vol. 102, pp. 110-118, 1980.

[25] D. Haemmerich ,S T Staelin ,J Z Tsai, S Tungjitkusolmun, D M Mahvi, and J G Webster,"In vivo electrical conductivity of hepatic tumours," *Insttute of Physics Publishing, Physiol. meas.,* pp.251-260, 2003

S. Tungjitkusolmun was born in Bangkok, Thailand, December 5, 1972. He received the B.S.E.E. degree from the University of Pennsylvania, Philadelphia, in 1995, and the M.S.E.E. and Ph.D. degrees from the University of Wisconsin, Madison, in 1996, and 2000, respectively. He is an Assistant Professor at the Department of Electronics, Faculty of Engineering, King Mongkut's Institute of Technology Ladkrabang, Bangkok, From 2003 to 2007, he was the Assistant Director, Computer Research and Service Center, King Mongkut's Institute of Technology Ladkrabang, Bangkok, Thailand. His research interests include finite-element modeling, radiofrequency ablation, microwave ablation, signal processing and image processing.